Damage Morphologies in Targets Exposed to a New Plasma Deflagration Accelerator for ELM Simulation

Keith T. K. Loebner, Thomas C. Underwood, Benjamin C. Wang, and Mark A. Cappelli

***Abstract*— Transient events in fusion power plants such as DEMO and ITER are known to pose a severe threat to plasma facing components (PFCs) due to melting and erosion after repeated edge localized mode (ELM) loads. *In situ* experimental testing of potential PFC materials at fusion relevant conditions is difficult and expensive, and as a result plasma devices capable of replicating the desired transient conditions are of increasing interest. At Stanford University, an experimental facility designed to mimic the heat flux, particle fluence, and other key characteristics of ELMs and disruption events in a controlled setting has been developed. A pulsed plasma accelerator operating in the deflagration mode is used to generate high-velocity (40–100 km/s) directed plasma jets that are stagnated on target material samples. In this paper, we present probe data characterizing the plasma parameters of the accelerated plume using hydrogen as the working gas, as well as preliminary target studies of silicon and copper witness plates exposed to pulses at various total and peak shot energies. Results from the probe analysis indicate achieved energy fluxes and heat flux parameters that are ELM-like, and the observed linearly correlated damage morphologies on the witness plates indicate that initial surface roughness plays a significant role in the growth characteristics of surface damage patterns. These results lay the groundwork for future studies of ELM-like loading on reactor-relevant materials using the Stanford plasma accelerator facility.**

***Index Terms*— Divertor material, erosion, first wall, off-normal events, plasma jet, plasma–material interaction (PMI), plasma–material interface.**

I. Introduction

AS INTERNATIONAL experimental fusion reactor facilities move closer toward operational status, attention is turning to the next generation of reactor designs and materials for practical power plants. One of the key engineering challenges in this development is the identification and understanding of the processes occurring at the interface between the plasma exhaust and the reactor first wall, as it is these phenomena that drive the suitability and lifetime of plasma facing components (PFCs) in the reactor, as well as whether the reactor is able to achieve the necessary confinement conditions.

It is known that the bulk of the transient loading experienced by PFCs is the result of edge localized modes (ELMs) and disruption events. As it is difficult to isolate these transient loads in an operating experimental reactor, other techniques have been devised for studying the interaction between plasmas at ELM-like conditions and materials often found in PFCs. These include the use of plasma guns, laser irradiation, and charged particle beams to produce high heat and/or particle fluxes directed onto a target substrate [1]–[5]. The latter two techniques can provide heat flux parameters of the order of those expected in ELMs, but may not capture the complex effects that result from a quasi-neutral plasma acting as the source of the energy flux. The former technique is the platform that we have chosen to develop at Stanford University, as it is the most flexible and appropriate analog to the conditions experienced in practical fusion machines (as demonstrated in [1] and [6]–[12]). By coupling detailed knowledge of the plasma environment both in the jet and in the vicinity of the target material, the potential exists for a significantly deeper understanding of the plasma–material interactions (PMIs) and the plasma edge physics, which play a critical role in fusion engineering.

In this paper, we report on the suitability of the Stanford Plasma Gun (SPG) experiment, which is a pulsed plasma accelerator operating in the deflagration regime described extensively in [1] and [13]–[16], for use as an analog plasma source designed to replicate ELM-like conditions and behavior. The SPG consists of a circularly arranged set of stainless-steel rod anodes, arrayed around a central copper cathode. There is an insulating sleeve around the rod anode array that serves to confine the gas as it is injected and accelerated, extending from the breach end up to the last 3 cm of the electrodes. A 56-μF capacitor bank charged to 3 kV was used as the driving circuit for the discharge. In order to fire the SPG, the electrode region is initially evacuated, and when the neutral gas is injected the field in the gap approaches the breakdown field from the vacuum side of the Paschen curve. More details on the construction and operation of the SPG can be found in [17]–[24]. We used a quadruple Langmuir probe (QLP) technique to perform low-energy parameter measurements in the plasma plume produced by the SPG, using hydrogen as the working gas. In particular, we obtained the energy flux and heat flux

Manuscript received July 31, 2015; revised February 22, 2016; accepted May 2, 2016. This work was supported by the U.S. Department of Energy National Nuclear Security Administration Stewardship Science Academic Program under Grant DE-NA0002011. The work of K. T. K. Loebner, T. C. Underwood, and B. C. Wang was supported by the National Defense Science and Engineering Graduate Fellowship under Grant 32 CFR 168a.

The authors are with the Department of Mechanical Engineering, Stanford University, Stanford, CA 94305 USA (e-mail: kloebner@stanford.edu).

Color versions of one or more of the figures in this paper are available online at http://ieeexplore.ieee.org.

Digital Object Identifier 10.1109/TPS.2016.2565508

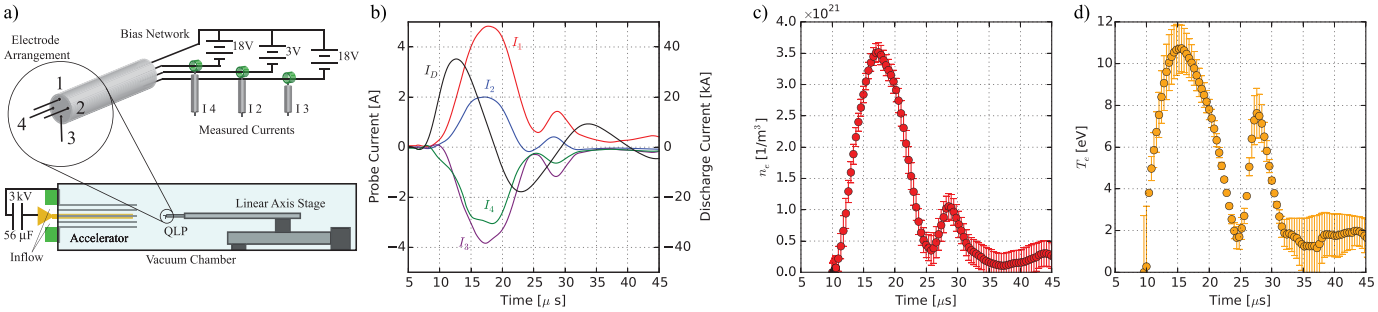

Fig. 1. (a) Schematic of the probe construction, bias network, and the probe installed on the linear axis stage in the vacuum chamber along with the SPG. Electrodes 1, 2, and 4 are oriented parallel to the plasma flow during machine operation. (b) Example current traces collected from the QLP as well as the corresponding discharge current trace (alternate y-axis). (c) Calculated time series of the plasma density based on the measured currents. (d) Calculated time series of the plasma temperature based on the measured currents.

parameter of the jet as a benchmark to compare against known ELM behavior [25], [26], by probing the plasma parameters in a manner similar to that described in [27]. Off-normal heat fluxes are considered (for current and next-step machines) to be those that are >20 MW $\cdot$ m^{-2}, with streaming plasma densities of $<10^{22}$ m^{-3} (to avoid shocks and vapor shielding at the plasma–material interface) [25]; our goal is to achieve parameters within this range.

We then performed a set of target studies using two different witness plate materials. The first set of target data was collected from a series of individual shots at the same charging energy, using polycrystalline silicon wafers. The results of these shots were analyzed via scanning electron microscopy (SEM). We then performed a two-parameter target study using copper witness plates, in which we vary the peak and integrated fluxes independently in order to determine which drives the degree and character of the resulting material damage. The copper witness plate samples are analyzed using a high-powered optical microscope with <1-μm resolution. From the combination of these two studies, we show that the observed damage appears to be strongly tied in type and severity to the peak fluxes, and that the morphology of the damage is closely linked to the initial surface characteristics and material of the target sample.

II. Plume Characterization

In the context of this paper, the primary goal of the plume characterization is to obtain a measurement of the bulk heat and particle fluxes experienced by the target surfaces. These measured parameters enable the observed effects on material surfaces to be closely coupled to the plasma conditions, instead of relying on estimates based upon the input energy to the accelerator. To this end, a QLP was used to obtain the plume parameters necessary to calculate a total energy flux and heat flux parameter to use as a benchmark for comparison against other plasma gun target studies in the literature, well summarized in [25].

A QLP is an immersed diagnostic tool that enables simultaneous time-resolved measurements of the plasma density, temperature, potential, and ion Mach number at the point location of the probe in the downstream region of the accelerator. The QLP was mounted to a linear axis stage, and by moving the probe along the axis over the course of multiple firings we were able to compile a spatiotemporal contour of each of the plasma state variables (see [21], [22], [24] for contour plots). For this study, the probe was operated in the current-saturation mode to obtain time-resolved measurements of the resulting plasma plume [28]. The probe as constructed consists of four independent electrodes, as shown in Fig. 1(a). Electrodes 1, 2, and 4 are oriented parallel to the flow direction while electrode 3 is perpendicular to the flow direction. Electrodes 3 and 4 are nominally biased at -18 V with respect to electrode 1 (ϕ_{13} and ϕ_{14}) while electrode 2 is biased at -3 V (ϕ_{12}).

In order to calculate the four independent plasma state variables, the measured current and associated bias voltages must be coupled with a theory describing the current collected by the probe surface. Similar to other electrostatic plasma probes, the collected probe current I_p is composed of contributions due to both electrons and ions and can be written as

$$I_p = I_e - I_i \tag{1}$$

where I_e and I_i correspond to electron and ion current, respectively. For any electrode exposed to the plasma flow, the collected current will correspond to electron flux if the probe potential is less than the plasma potential ($\phi_{\text{probe}} \leq \phi_{\text{plasma}}$) according to the expression

$$I_{\|e} = A_{\text{probe}} J_{e0} \exp\left[-\frac{e}{kT}(\phi_{\text{plasma}} - \phi_{\text{probe}})\right] \tag{2}$$

which is a function of the probe area both parallel and/or perpendicular to the plasma flow direction, A_{probe}, and the thermal diffusion of electrons. Current due to ion collection, however, is a more complex function of the operating regime of the probe. More specifically, the ratio of the local probe radius to the Debye length, r_p/λ_D, and the ratio of ion to electron temperature, T_i/Z_iT_e, governs which theory should be applied. If $5 \leq r_p/\lambda_D \leq 100$ and $T_e/Z_iT_i \leq 1$, 29 developed a relationship for ion current collection as a function of the empirical fitting parameters α and β based upon experimental measurements [30]

$$I_{\|i} = A_{\text{probe}} J_{i0}\left(\beta + \frac{e}{kT}(\phi_{\text{plasma}} - \phi_{\text{probe}})\right)^{\alpha} \tag{3}$$

$$\alpha = \frac{2.9}{\ln(r_p/\lambda_D) + 2.3} + 0.07\left(\frac{T_i}{Z_iT_e}\right)^{0.75} - 0.34 \tag{4}$$

$$\beta = 1.5 + \frac{T_i}{Z_iT_e}\left[0.85 + 0.135\left(\ln\left[\frac{r_p}{\lambda_D}\right]\right)^3\right]. \tag{5}$$

An analytical expression for the ion current collected by the perpendicular probe in particular was obtained by assuming a negligible sheath thickness [31], i.e., $d_s/r_p \to 1$, such that

$$I_{\perp i} = A_\perp n_e e \left(\frac{kT}{2\pi m_e}\right)^{1/2} \frac{2}{\sqrt{\pi}} \exp\left[-S_i^2\right] \times \sum_{j=0}^{\infty} \frac{S_i^j}{j!} \Gamma\left(j+\frac{3}{2}\right). \quad (6)$$

Coupling these expressions with the assumptions of quasi-neutrality ($n_e = n$) and thermal equilibrium ($T_i = T_e$) between the electron and ion plasma components, a set of four coupled nonlinear equations for the desired parameters can be developed, giving

$$I_1 = A_\parallel J_{e0} \exp\left(-\frac{e\phi_{p1}}{kT}\right) - A_\parallel J_{i0} \left(\beta + \frac{e\phi_{p1}}{kT}\right)^{\alpha} \quad (7)$$

$$I_2 = A_\parallel J_{e0} \exp\left(-\frac{e(\phi_{p1}+\phi_{12})}{kT}\right) - A_\parallel J_{i0} \left(\beta + \frac{e(\phi_{p1}+\phi_{12})}{kT}\right)^{\alpha} \quad (8)$$

$$I_3 = A_\parallel J_{e0} \exp\left(-\frac{e(\phi_{p1}+\phi_{13})}{kT}\right) - A_\parallel J_{i0} \left(\beta + \frac{e(\phi_{p1}+\phi_{13})}{kT}\right)^{\alpha} \quad (9)$$

$$I_4 = A_\perp J_{e0} \exp\left(-\frac{e(\phi_{p1}+\phi_{14})}{kT}\right) - A_\perp n_e e \left(\frac{kT}{2\pi m_e}\right)^{1/2} \frac{2}{\sqrt{\pi}} \exp\left(-S_i^2\right) \times \sum_{j=0}^{\infty} \frac{S_i^j}{j!} \Gamma\left(j+\frac{3}{2}\right) \quad (10)$$

where ϕ_{ij} is the potential between electrodes i and j (and subscript p is the plasma), S_i is the ion thermal Mach number, $A_\parallel$ and $A_\perp$ are the probe areas parallel and perpendicular to the flow, respectively, k is the Boltzmann constant, and T is the plasma temperature. These equations are solved at each recorded data point in time to obtain a time series of the derived plasma parameters in a single shot. In the event that $r_p/\lambda_D > 100$, the ion collection theory used in (3) is invalid. In this case, a thin sheath is assumed and the ion current follows a Bohm expression [32]:

$$I_{\parallel i} = A_\parallel n_e e \sqrt{\frac{kT}{m_i}} \exp\left(-\frac{1}{2}\right). \quad (11)$$

Incorporation of this thin sheath assumption leads to the following revised set of current balance equations, valid for a thin sheath $r_p/\lambda_D > 100$:

$$I_1 = A_\parallel J_{e0} \exp\left(-\frac{e\phi_{p1}}{kT}\right) - A_\parallel n_e e \sqrt{\frac{kT}{m_i}} \exp\left(-\frac{1}{2}\right) \quad (12)$$

$$I_2 = A_\parallel J_{e0} \exp\left(-\frac{e(\phi_{p1}+\phi_{12})}{kT}\right) - A_\parallel n_e e \sqrt{\frac{kT}{m_i}} \exp\left(-\frac{1}{2}\right) \quad (13)$$

$$I_3 = A_\parallel J_{e0} \exp\left(-\frac{e(\phi_{p1}+\phi_{13})}{kT}\right) - A_\parallel n_e e \sqrt{\frac{kT}{m_i}} \exp\left(-\frac{1}{2}\right) \quad (14)$$

$$I_4 = A_\perp J_{e0} \exp\left(-\frac{e(\phi_{p1}+\phi_{14})}{kT}\right) - A_\perp n_e e \left(\frac{kT}{2\pi m_e}\right)^{1/2} \frac{2}{\sqrt{\pi}} \exp\left(-S_i^2\right) \times \sum_{j=0}^{\infty} \frac{S_i^j}{j!} \Gamma\left(j+\frac{3}{2}\right). \quad (15)$$

The systems described by (7)–(10) and (12)–(15) are solved using a standard Newton–Raphson algorithm with a centered trust region. The initial guess of each state variable provided to the solver are obtained by solving the algebraically reduced system that provides a first-order solution of the derived plasma parameters. In order to ensure that the correct ion collection model is used for each data point, the system of equations corresponding to the thin sheath assumption is solved first and the resulting Debye length is computed. If r_p/λ_D is such that the theory developed in [30] is valid, the state variables are recalculated using the equations corresponding to the empirical fit.

A. Results

The probe data was collected at 19 spatial points, ranging from 70–160 mm from the exit plane of the accelerator. The resulting spatiotemporal contour for plasma density is used to obtain the plume velocity by way of time-of-flight, as detailed in [23]. Using only the density and temperature contours, and estimating the bulk plasma velocity via the slope of the leading edge of the plasma density contour, we calculate the relevant bulk energy flux and heat flux parameter for the jet. These data were collected only for the 3-kV charging voltage, corresponding to 252 J/pulse, due to the fact that at higher energies it was not technically feasible to collect probe data this close to the exit plane of the accelerator as a result of arcing. Scaling of the plasma parameters with machine operating conditions is explored in other work (see [21], [23]), but the key state variables (i.e., density and temperature) scale approximately with the square of the peak current (and, thus, with the magnetic pressure) while the velocity scales approximately linearly with charging voltage (and, thus, with peak current). This allows for estimation of the expected conditions at a material target for a range of machine operating points.

The validity of the QLP measurements depends upon the probe theory being consistent with the physical regime of the plasma (e.g., the extent to which quasi-neutrality is valid in the vicinity of the probe), as well as the degree of magnetization and local thermal equilibrium. The calculated plasma parameters are used to determine whether the validity criteria described above for the probe theory have been met, as a check against arriving at a mathematically convergent solution that is nevertheless physically unrealistic; these calculations show that we are indeed operating in the appropriate regime for

the QLP. Without a direct measurement of the magnetic field density in the plasma plume, we cannot definitively state that the plasma plume is unmagnetized at the locations of the probe measurements. However, a theoretical model for the operation of the deflagration mode (detailed extensively in [21]) shows that very little, if any, magnetic flux is convected downstream of the SPG. Finally, thermal equilibrium between the electron and ion species has been shown to be present in similar devices (see [10], [12]), and spectroscopic studies of the SPG (see [23]) show that there is local thermodynamic equilibrium between the various constituents of the plasma. Example calculated traces are shown in Fig. 1(c) and (d), with error bars calculated from a sensitivity study of the probe behavior over a series of SPG firings at the same operating condition (see [21]).

The energy flux ($\mathscr{E}$) is assumed to consist entirely of the internal energy (i.e., the kinetic temperature) of the flowing plasma and the kinetic energy carried by the plasma jet. This is calculated as

$$\mathscr{E} = \tilde{c}_v T_e \cdot n_e V + \frac{1}{2} m_p V^2 \cdot n_e V \tag{16}$$

where $\tilde{c}_v$ is the per-particle heat capacity of hydrogen at constant volume [assumed to be $(3/2)k_B$], T_e is the plasma temperature (where we have assumed that $T_e = T_i$ as per the QLP theory), m_p is the proton mass, n_e is the plasma density, and V is the bulk jet velocity. Using the nominal values from the probe data of $T_e \simeq 10$ eV, $n_e \simeq 10^{21}$ m^{-3}, and $V \simeq 40$ km/s (obtained via the slope of the leading edge of the spatiotemporal contour), we obtain an energy flux of

$$\mathscr{E} \simeq 150 \text{ MW m}^{-2}.$$

For a nominal pulse with of $\sim$10 μs (obtained from the width of the plasma pulse in the contours), the heat flux parameter ($\mathscr{H}$) is thus

$$\mathscr{H} = 0.58 \text{ MJ m}^{-2} \text{ s}^{-1/2}.$$

This is somewhat lower than the heat flux parameter typically used to replicate ELMs in systems developed by others [3]. However, this apparent shortcoming is mitigated for two reasons.

1) This heat flux parameter is based on the measured data in the plasma plume, so it is not immediately apparent that this is in fact a significantly lower number than that actually realized by systems based on optical heating, given the lack of actual heat flux data in those cases.
2) We expect the heat flux parameter to scale approximately linearly with the input energy, and these data were collected at a comparatively low input energy ($\sim$250 J/pulse).

The heat flux parameter is therefore likely to be in the range of 4.1 MJ $\cdot$ m$^{-2} \cdot$ s$^{-1/2}$ at the highest pulse energy tested in this study. Furthermore, the overall energy flux is higher than that generally associated with ELMs, and thus multiple firings should be able to achieve a higher effective heat flux parameter (by increasing the effective period) while still maintaining the minimum energy flux to replicate ELM-like damage in material targets.

We also note that the plasma temperatures measured in the plume are much lower than what would be expected in a large tokamak (a pedestal electron temperature of $\sim$2–4 keV is thought necessary for optimal ITER performance [33]). This limitation is difficult to overcome in relatively small plasma sources such as the SPG, and efforts to increase the plasma temperature using external sources (such as pulsed bias fields) often comes at the expense of directed kinetic energy and velocity (see [34]), reducing the overall particle and energy fluxes. In addition, the authors recognize that the near-field magnetic topology of the SPG is similar to a continuous-flow Z-pinch, and thus substantially different from that in the vicinity of a tokamak divertor under typical configurations [35], [36]. However, PMI dynamics that are governed by the total energy and heat fluxes, more so than the ion or electron temperatures themselves and/or the particular magnetic field configuration, are well within the experimental reach of systems such as the SPG.

III. Witness Plate Target Studies

In an effort to determine the type and degree of damage caused by the accelerated plasma jets, a series of experiments using witness plates was performed as a means of investigating the bulk effects of the jet on the sample. The first set of targets used were polycrystalline silicon wafers, placed normal to the flow direction along the central axis of the accelerator. The second set of targets used were unpolished, mirror-finish pure copper tokens, also placed normal to the flow direction along the central axis of the accelerator. In each case, the target was located $\sim$10 cm from the exit plane of the accelerator, and held in a sample holder mounted to the linear axis stage; the stage was kept at the same position for all the trials. The stage was isolated from any external electronics, and the samples were electrically isolated from the stage, such that the targets were allowed to float relative to the plasma potential and the ground.

The objective of this paper was twofold.

1) To establish a baseline characterization of whether the facility can produce observable damage on a target substrate.
2) To preliminarily investigate whether the aggregate energy delivered to the target or the peak energy flux drives the scale and qualitative aspects of the observed damage.

A. Results: Silicon Targets

The first set of shots was performed using polycrystalline silicon wafers. A series of representative SEM images, depicting typical damage morphologies and observed features, is shown in Fig. 2.

There is clear evidence of large voids that could be produced by macroparticles entrained by the plasma jet, but there are no obvious indications of surface melting. The depth of the macroparticle bore into the sample is beyond what is resolvable using the SEM, as shown in Fig. 2(e). A single shot also produced small island-like features, visible in Fig. 2(c), which we interpret to be either redeposited silicon material from elsewhere on the wafer or deposited ablated material

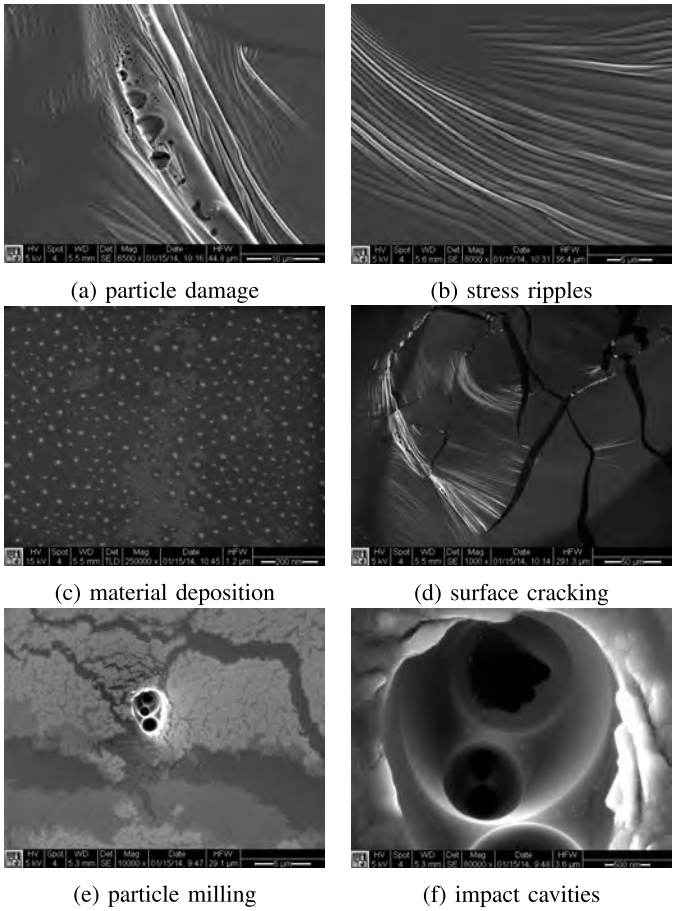

Fig. 2. SEM images of observed material damage on Si wafers after exposure to a single 6-kV shot. (a)–(e) Correspond to the same magnification (scale bar visible). (f) Ten times greater magnification of the image from (e).

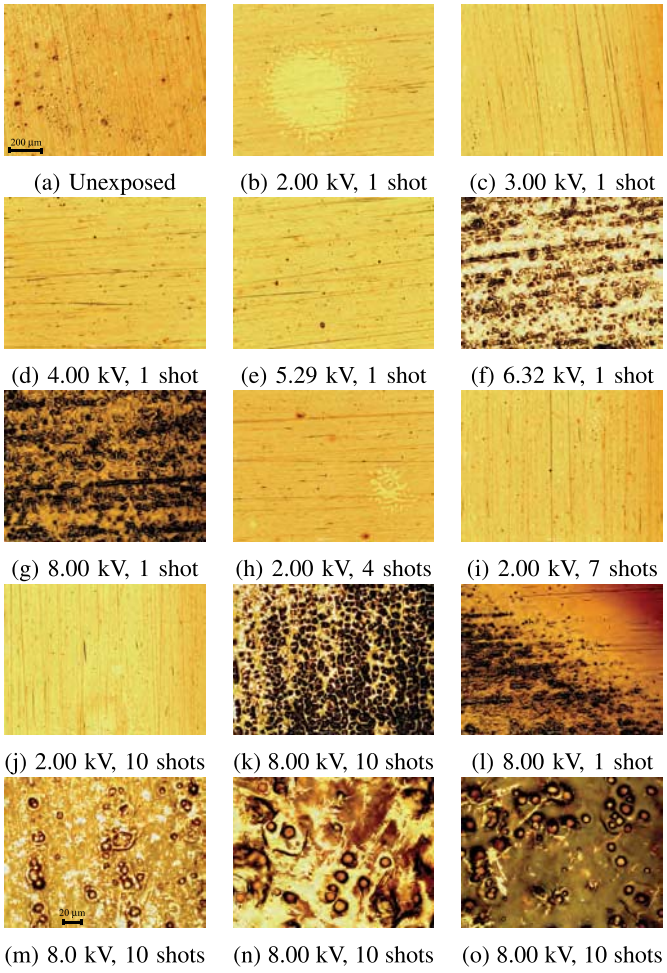

Fig. 3. Compilation of optical micrographs of damage to Cu tokens corresponding to all the tested conditions in the witness plate study. (a)–(l) Correspond to the same magnfication (scale bar visible). (m)–(o) Images taken at ten times greater magnification.

from the accelerator itself. The stress ripples and surface cracking shown in Fig. 2(b) and (d) show that significant mechanical stress is being generated in the surface layers of the target. These results indicate that the plasma environment produced by the SPG is capable of producing material damage in crystalline targets that can be observed and related back to the plasma source; however, since metallic targets are more representative of the actual PFCs in a reactor and have substantially different bulk properties than Si, a more detailed study using copper targets was also conducted. Though copper itself is unlikely to be a plasma facing material, the relationship between observable damage morphologies (e.g., melting) and energy flux is well characterized for copper, making it a suitable material choice without *a priori* knowledge of what the effects of the plasma might be on a more robust target material (e.g., tungsten).

B. Results: Copper Targets

The optical micrographs of the series of targets irradiated by the SPG facility are shown in Fig. 3. Since the copper targets were not additionally polished beyond the stock mirror finish prior to exposure, the initial surface characteristics displayed a fairly large degree of initial roughness on the microscale [shown in Fig. 3(a)] due to residual machining marks. However, this led to what is one of the more interesting results of the target study: the damage from the impinging plasma jet was observed to localize preferentially along the linear grooves in the material. Examples of this are clearly visible in Fig. 3(f), (g), and (l). The latter micrograph shows the boundary between the exposed and unexposed portions of the witness plate, where the transition from unexposed linear grooves to linearly structured damage zones is clearly visible.

The additional objective of the target study was to determine whether the total energy flux, i.e., over multiple low-energy shots, would achieve the same types of damage generated by a single high-energy-flux shot. As is clearly visible from the micrographs, equivalent total energy fluxes do not produce the same results. For example, the SPG fired ten times at 2.0 kV [Fig. 3(j)] corresponds to the same total energy flux as the SPG fired at 6.32 kV a single time [Fig. 3(f)]. This comparison assumes that the actual energy flux in the jet correlates to the initially stored energy in the capacitor bank, but it is evident that even if there is a moderately nonlinear scaling of the jet parameters with energy, the damage sustained is much more strongly dependent on the peak fluxes experienced by the target.

IV. Conclusion

We have presented a study that provides preliminary indications that the SPG facility is suitable for generating ELM-like loads for testing candidate PFC materials and configurations. The tested configurations were confined to normal-incidence impacts of the plasma jet onto the target surface, but the facility is easily adaptable to oblique incidence angle configurations, grouped targets with fixed separation (as in the ITER divertor cassettes), and other such configurations. Although the overall fluence and energy density remains somewhat below that expected for single ELM events in the regimes tested, the peak fluxes are sufficiently large at high energy (>1 kJ/pulse), so that the shortcoming in the total energy deposition can be mitigated over the course of multiple firings. Furthermore, the facility is capable of operating at maximum energies of 12 kJ/pulse, i.e., one order of magnitude higher input energy, and thus the predicted energy densities for ELM events are at least theoretically attainable over the course of a single shot.

The data collected via the QLP enabled the calculation of the direct plasma parameters necessary to determine the bulk energy flux of the jet, and the target studies indicated that achieving the requisite damage threshold is a strong function of the peak energy flux. The target studies also provided a promising avenue for further work, studying the specific mechanism responsible for damage localization at the initial sites of surface irregularity. One explanation is the reduced ability of the substrate to conduct heat away from the increased surface area in the vicinity of the groove, as well as increased field electron emission from the surface in the vicinity of the sharp groove edges driving higher ion fluxes into the surface. This interesting result reinforces the fact that the proper evaluation of potential PFCs under fusion conditions requires the use of high-energy plasma sources such as the SPG facility, in order to capture the complex interaction of the plasma and material interface. In the future work, we will expand the selection of PFC targets to include materials of greater relevance to fusion systems, such as pure tungsten, tungsten alloys, and carbon-containing materials.

References

[1] J. T. Bradley, III, J. M. Gahl, and P. D. Rockett, "Diagnostics and analysis of incident and vapor shield plasmas in PLADIS I, a coaxial deflagration gun for tokamak disruption simulation," *IEEE Trans. Plasma Sci.*, vol. 27, no. 4, pp. 1105–1114, Aug. 1999.

[2] G. Federici *et al.*, "Effects of ELMs and disruptions on ITER divertor armour materials," *J. Nucl. Mater.*, vols. 337–339, pp. 684–690, Mar. 2005. [Online]. Available: http://www.sciencedirect.com/science/article/pii/S0022311504009353

[3] I. E. Garkusha *et al.*, "The latest results from ELM-simulation experiments in plasma accelerators," *Phys. Scripta*, vol. T138, no. T138, p. 014054, 2009.

[4] S. Kajita, N. Ohno, S. Takamura, W. Sakaguchi, and D. Nishijima, "Plasma-assisted laser ablation of tungsten: Reduction in ablation power threshold due to bursting of holes/bubbles," *Appl. Phys. Lett.*, vol. 91, no. 26, p. 261501, Dec. 2007. [Online]. Available: http://scitation.aip.org/content/aip/journal/apl/91/26/10.1063/1.2824873

[5] T. Hirai *et al.*, "Characterization and heat flux testing of beryllium coatings on Inconel for JET ITER-like wall project," *Phys. Scripta*, vol. T128, no. T128, pp. 166–170, Mar. 2007. [Online]. Available: http://iopscience.iop.org/article/10.1088/0031-8949/2007/T128/032

[6] P. D. Rockett, J. A. Hunter, J. M. Gahl, J. T. Bradley, III, and R. R. Peterson, "Plasma gun experiments and modeling of disruptions," *J. Nucl. Mater.*, vols. 212–215, pp. 1278–1282, Sep. 1994. [Online]. Available: http://www.sciencedirect.com/science/article/pii/0022311594910359

[7] U. Shumlak, B. A. Nelson, R. P. Golingo, S. L. Jackson, E. A. Crawford, and D. J. Den Hartog, "Sheared flow stabilization experiments in the ZaP flow Z pinch," *Phys. Plasmas*, vol. 10, no. 5, p. 1683, Apr. 2003. [Online]. Available: http://scitation.aip.org/content/aip/journal/pop/10/5/10.1063/1.1558294

[8] S. L. Jackson, "Density characteristics of a sheared-flow Z-pinch," Ph.D. dissertation, Dept. Aeron. Astron., Univ. Washington, Seattle, WA, USA, 2006. [Online]. Available: http://www.aa.washington.edu/research/ZaP/Publications/APS05_jackson.pdf

[9] M. J. Baldwin and R. P. Doerner, "Helium induced nanoscopic morphology on tungsten under fusion relevant plasma conditions," *Nucl. Fusion*, vol. 48, no. 3, p. 035001, Mar. 2008. [Online]. Available: http://iopscience.iop.org/article/10.1088/0029-5515/48/3/035001

[10] U. Shumlak *et al.*, "Equilibrium, flow shear and stability measurements in the Z-pinch," *Nucl. Fusion*, vol. 49, no. 7, p. 075039, Jul. 2009. [Online]. Available: http://iopscience.iop.org/article/10.1088/0029-5515/49/7/075039

[11] M. Miyamoto *et al.*, "Microscopic damage of tungsten exposed to deuterium–helium mixture plasma in PISCES and its impacts on retention property," *J. Nucl. Mater.*, vol. 415, no. 1, pp. S657–S660, Aug. 2011. [Online]. Available: http://www.sciencedirect.com/science/article/pii/S0022311511000201

[12] U. Shumlak *et al.*, "Long, stable plasma generation in the ZaP flow Z-pinch," in *Proc. Abstracts IEEE Int. Conf. Plasma Sci.*, Jul. 2012, p. 2P-94. [Online]. Available: http://ieeexplore.ieee.org/lpdocs/epic03/wrapper.htm?arnumber=6383650

[13] D. Y. Cheng, "Plasma deflagration and the properties of a coaxial plasma deflagration gun," *Nucl. Fusion*, vol. 10, no. 3, pp. 305–317, Sep. 1970. [Online]. Available: http://stacks.iop.org/0029-5515/10/i=3/a=011?key=crossref.653d85b404f52df711f900156dbf3e56

[14] D. M. Woodall and L. K. Len, "Observation of current sheath transition from snowplow to deflagration," *J. Appl. Phys.*, vol. 57, no. 3, p. 961, 1985. [Online]. Available: http://scitation.aip.org/content/aip/journal/jap/57/3/10.1063/1.334697

[15] R. J. Wallace, "Theoretical, computational and experimental analysis of the deflagration plasma accelerator and plasma beam characteristics," Ph.D. dissertation, Dept. Aerosp. Eng., Virginia Polytech. Inst. State Univ., Blacksburg, VA, USA, 1991. [Online]. Available: http://adsabs.harvard.edu/abs/1991PhDT.....197W

[16] Y. C. F. Thio *et al.*, "An experimental study of a low-jitter pulsed electromagnetic plasma accelerator," in *Proc. 38th AIAA/ASME/SAE/ASEE Joint Propuls. Conf. Exhibit*, Indianapolis, IN, USA, 2002, pp. 1–13. [Online]. Available: http://arc.aiaa.org/doi/pdf/10.2514/6.2002-4269

[17] K. Loebner, F. Poehlmann, and M. Cappelli, "Current distribution characterization and circuit analysis of a high energy pulsed plasma deflagration," *Bull. Amer. Phys. Soc.*, vol. 57, no. 8, p. 1084, Oct. 2012. [Online]. Available: http://meetings.aps.org/link/BAPS.2012.GEC.PR1.84

[18] K. T. K. Loebner, B. C. Wang, F. R. Poehlmann, Y. Watanabe, and M. A. Cappelli, "High-velocity neutral plasma jet formed by dense plasma deflagration," *IEEE Trans. Plasma Sci.*, vol. 42, no. 10, pp. 2500–2501, Oct. 2014. [Online]. Available: http://ieeexplore.ieee.org/lpdocs/epic03/wrapper.htm?arnumber=6849459

[19] K. Loebner, B. Wang, and M. Cappelli, "Experimental characterization of magnetogasdynamic phenomena in ultra-high velocity pulsed plasma jets," *Bull. Amer. Phys. Soc.*, vol. 59, no. 16, p. 2001, Nov. 2014. [Online]. Available: http://meetings.aps.org/link/BAPS.2014.GEC.SF2.1

[20] K. T. K. Loebner, T. C. Underwood, and M. A. Cappelli, "A fast rise-rate, adjustable-mass-bit gas puff valve for energetic pulsed plasma experiments," *Rev. Sci. Instrum.*, vol. 86, no. 6, p. 063503, 2015.

[21] K. T. K. Loebner, T. C. Underwood, and M. A. Cappelli, "Evidence of branching phenomena in current-driven ionization waves," *Phys. Rev. Lett.*, vol. 115, no. 17, p. 175001, Oct. 2015. [Online]. Available: http://link.aps.org/doi/10.1103/PhysRevLett.115.175001

[22] K. T. K. Loebner, T. C. Underwood, A. L. Fabris, M. A. Cappelli, and J. J. Szabo, "Plume characterization of gas-fed pulsed plasma deflagration thrusters," in *Proc. 34th Int. Electr. Propuls. Conf.*, Kobe, Japan, 2015, pp. 1–10.

[23] K. Loebner, T. Underwood, T. Mouratidis, and M. Cappelli, "Spectroscopic study of a pulsed high-energy plasma deflagration accelerator," *Bull. Amer. Phys. Soc.*, vol. 60, no. 19, p. 113, Nov. 2015. [Online]. Available: http://meetings.aps.org/link/BAPS.2015.DPP.GP12.49

[24] T. Underwood, K. Loebner, and M. Cappelli, "Experimental validation of a branched solution model for magnetosonic ionization waves in plasma accelerators," *Bull. Amer. Phys. Soc.*, vol. 60, no. 19, p. 176, Nov. 2015. [Online]. Available: http://meetings.aps.org/link/BAPS.2015.DPP.JP12.148

[25] G. Federici *et al.*, "Plasma-material interactions in current tokamaks and their implications for next step fusion reactors," *Nucl. Fusion*, vol. 41, no. 12, pp. 1967–2137, Dec. 2001. [Online]. Available: http://stacks.iop.org/0029-5515/41/i=12/a=218

[26] A. W. Leonard, "Edge-localized-modes in tokamaks," *Phys. Plasmas*, vol. 21, no. 9, p. 090501, Sep. 2014. [Online]. Available: http://scitation.aip.org/content/aip/journal/pop/21/9/10.1063/1.4894742

[27] S. Jung, V. Surla, T. K. Gray, D. Andruczyk, and D. N. Ruzic, "Characterization of a theta-pinch plasma using triple probe diagnostic," *J. Nucl. Mater.*, vol. 415, no. 1, pp. S993–S995, 2011.

[28] N. A. Gatsonis, J. Zwahlen, A. Wheelock, E. J. Pencil, and H. Kamhawi, "Characterization of a pulsed plasma thruster plume using a quadruple Langmuir probe method," in *Proc. 38th AIAA/ASME/SAE/ASEE Joint Propulsion Conf. Exhibit*, vol. 4123. Indianapolis, IN, USA, Jul. 2002, p. 2002.

[29] E. W. Peterson and L. Talbot, "Collisionless electrostatic single-probe and double-probe measurements," *AIAA J.*, vol. 8, no. 12, pp. 2215–2219, 1970.

[30] J. Laframboise, "Theory of cylindrical and spherical Langmuir probes in a collisionless plasma at rest," in in *Proc. 4th Int. Symp. Rarefied Gas Dyn.*, vols. 1–2. Toronto, ON, Canada, 1964, p. 22.

[31] B. H. Johnson and D. L. Murphree, "Plasma velocity determination by electrostatic probes," *AIAA J.*, vol. 7, no. 10, pp. 2028–2030, 1969.

[32] S.-L. Chen and T. Sekiguchi, "Instantaneous direct-display system of plasma parameters by means of triple probe," *J. Appl. Phys.*, vol. 36, no. 8, pp. 2363–2375, 1965.

[33] A. W. Leonard *et al.*, "The impact of ELMs on the ITER divertor," *J. Nucl. Mater.*, vols. 266–269, pp. 109–117, Mar. 1999. [Online]. Available: http://www.sciencedirect.com/science/article/pii/S0022311598005224

[34] S. Jung, M. Christenson, D. Curreli, C. Bryniarski, D. Andruczyk, and D. N. Ruzic, "Development of a high energy pulsed plasma simulator for the study of liquid lithium trenches," *Fusion Eng. Design*, vol. 89, no. 12, pp. 2822–2826, Dec. 2014. [Online]. Available: http://www.sciencedirect.com/science/article/pii/S0920379614001586

[35] K. T. K. Loebner, T. C. Underwood, T. Mouratidis, and M. A. Cappelli, "Radial magnetic compression in the expelled jet of a plasma deflagration accelerator," *Appl. Phys. Lett.*, vol. 108, no. 9, p. 094104, Mar. 2016. [Online]. Available: http://scitation.aip.org/content/aip/journal/apl/108/9/10.1063/1.4943370

[36] A. E. Prinn and B. W. Ricketts, "Experimental study of a continuous flow pinch," *J. Phys. D, Appl. Phys.*, vol. 5, no. 11, p. 2026, 1972. [Online]. Available: http://iopscience.iop.org/0022-3727/5/11/309

Keith T. K. Loebner received the B.S. degree in aerospace engineering from the Massachusetts Institute of Technology, Cambridge, MA, USA, in 2011, and the M.S. degree in mechanical engineering from Stanford University, Stanford, CA, USA, in 2013, where he is currently pursuing the Ph.D. degree with the Mechanical Engineering Department.

He has conducted summer research projects with the Lawrence Livermore National Laboratory, Livermore, CA, USA, and the Naval Post-Graduate School, Monterey, CA, USA, in 2012 and 2013, respectively. His current research interests include high energy pulsed plasmas, fusion energy and enabling technologies, magnetohydrodynamics, and plasma–material interactions.

Thomas C. Underwood received the B.S. degrees in physics and nuclear engineering from the University of Florida, Gainesville, FL, USA, in 2014, and the M.S. degree in mechanical engineering from Stanford University, Stanford, CA, USA, in 2016, where he is currently pursuing the Ph.D. degree with the Mechanical Engineering Department.

His current research interests include atmospheric pressure dielectric-barrier discharges, pulsed plasmas, and Vlasov plasma modeling.

Benjamin C. Wang received the B.A. (Hons.) degree in physics and the B.A. degree in economics from the University of North Carolina at Chapel Hill, Chapel Hill, NC, USA, in 2011, and the M.S. degree in mechanical engineering from Stanford University, Stanford, CA, USA, in 2014, where he is currently pursuing the Ph.D. degree with the Mechanical Engineering Department.

His current research interests include plasma–material interactions and plasma-based microwave circuits and devices.

Mark A. Cappelli received the B.A.Sc. degree in physics from McGill University, Montréal, QC, Canada, in 1980, and the M.A.Sc. and Ph.D. degrees in aerospace science and engineering from the University of Toronto, Toronto, ON, Canada, in 1983 and 1987, respectively.

He is currently a Professor with the Department of Mechanical Engineering, Stanford University, Stanford, CA, USA. His current research interests include broad aspects of plasmas and gas discharges as they apply to aerodynamic and space propulsion, combustion, electromagnetics, and material processing.